MULTIPLE TRANSITION MODE MULTIPLE TARGET TRACK-BEFORE-DETECT WITH PARTITIONED SAMPLING

Samuel P. Ebenezer and Antonia Papandreou-Suppappola

School of Electrical, Computer, and Energy Engineering, Arizona State University, Tempe, Arizona 85287
Emails: esamuel@asu.edu and papandreou@asu.edu

ABSTRACT

In this paper, we extend the multiple model track-before-detect method to track all possible target combinations at low signal-to-noise ratios. Given a maximum number of targets, the method estimates the posterior probability density function of the multi-target state vector, the corresponding target existence probabilities, and the probabilities of all possible target combinations. As the particle filter implementation of this method requires a large number of particles to achieve high tracking performance, we propose an efficient partition based proposal function method by partitioning the multiple target space into a set of single target spaces. We also integrate the Markov chain Monte Carlo Metropolis-Hastings method into the particle proposal process to improve sample diversity. The proposed algorithm is validated by tracking five targets in very low signal-to-noise ratios (SNRs).

I. INTRODUCTION AND PRIOR WORK

Tracking multiple targets is a very challenging problem, especially at low SNRs. In addition to recovering data associations between targets and multiple observations, a process complicated by low probability of target detection due to low SNRs, operating in high clutter conditions causes increases in the number of false alarms. Different multi-target tracking methods were developed, including multiple hypothesis tracking and joint probabilistic data association [1] and probability hypothesis density filtering [2]; these methods assume that the targets are highly-observable. Track-before-detect (TBD) is a method proposed to improve tracking under low SNR conditions. It uses unthresholded data and a binary target existence variable into the target state estimation process. As it can be implemented by a particle filter (PF), it can be shown to be computationally feasible [3]. A recursive PF-TBD algorithm for a single target was introduced in [4] using the interactive multiple model (IMM) [3], [5]. Following this method, the TBD was used for multiple target tracking [6], [7]. In [8], the TBD was integrated with the probability hypothesis density filter (PHDF) for tracking multiple targets (PHDF-TBD). PHDF-based multi-target TBD algorithms were also developed in [9]–[11]. The poor performance of the PHDF-TBD in [8] was demonstrated for tracking three well-separated targets, and the use of multiple independent measurements from multiple homogeneous sensors was proposed to improve the PHDF-TBD tracking performance [11]. The PHDF-TBD algorithms in [9], [10] were only demonstrated by tracking two targets. All these aforementioned methods require an extra clustering step for track management for the sequential Monte-Carlo (SMC) based implementation of the PHDF [12].

In [13], we proposed an SMC-based multiple-target multiple mode TBD approach (MMMT-TBD) method for tracking multiple targets using different modes to correspond to different target combinations. This method generalizes the recursive and multiple model TBD [4], [14] algorithm to track multiple targets while keeping track of targets entering and leaving the field-of-view (FOV) at any given time step. In [14], a restrictive example was provided for tracking a second target that spawns from the first target; this method does not, however, include all possible combinations of targets leaving and entering a scene as it does not have an unambiguous mechanism to track the trajectory of the remaining targets after one of the targets leaves the scene.

The SMC based implementation of the MMMT-TBD requires a large number of particles to achieve high tracking performance. In this paper, we propose a partition based method to improve the tracking performance of the MMMT-TBD using a smaller number of particles. The multi-target space is partitioned into a set of single target spaces to generate proposal particles, and the measurement is used to select only high likelihood particles from a set of particles generated from a single target space partition. We also integrate the MCMC Metropolis-Hastings method [3] into the proposal particle generation step to reduce sample impoverishment.

This paper is organized as follows. In Section II, we provide the state and measurement models for the multiple transition mode multiple target TBD (MMMT-TBD). We develop the MMMT-TBD in Section III, and we provide its PF implementation in Section IV. We propose the independent sample partitioning based MMMT-TBD using MCMC in Section V. Simulation results comparing the various methods are discussed in Section VI.

II. MULTIPLE TARGET TBD TRACKING MODEL

When estimating multiple target parameters using TBD, the state model must consider all possible target combinations. In general, for a given maximum number of targets $\mathtt{L}$, the total number of target combinations or modes is $M = \sum_{\ell=0}^{\mathtt{L}} \mathtt{L}!/(\ell!(\mathtt{L}-\ell)!)$. This model enables the detection of a target entering the FOV (*target birth*) or exiting the FOV (*target death*) while tracking a different surviving target. For example, there are 4 possible modes for $\mathtt{L}=2$ targets: (a) no target is present; (b) only first target is present; (c) only second target is present; (d) both targets are present. Using the MMMT-TBD we proposed in [13], we also estimate the mode dynamic state and the joint probability density function (PDF) of the multi-target state vector. At time step k, we model the random mode transition as an M-state first order Markov chain $m_k \in \{0, 1, \ldots, M-1\}$. An $(M \times M)$ state mode transition matrix $\mathbf{\Phi}$ is constructed assuming known probabilities $\mathrm{Pr}_{\mathrm{B},\ell}$ and $\mathrm{Pr}_{\mathrm{D},\ell}$ of ℓ targets entering and exiting the FOV, respectively. The elements of $\mathbf{\Phi}$ are calculated based on the target combinations at time steps (k-1) and k. For example, if the targets are moving independently, the probability of switching from mode $m_{k-1}=1$ (one target present) to mode $m_k = M-1$ (all targets present) is $(1-\mathrm{Pr}_{\mathrm{D},1})\,\mathrm{Pr}_{\mathrm{B},\mathtt{L}-1}$.

978-1-4799-2893-4/14/$31.00 ©2014 IEEE

As the number of targets present varies for different modes, the state vector in mode i is represented as $\mathbf{x}_k^{(i)}$. For example, if the first and third targets are present in mode i, the multi-target state vector is $\mathbf{x}_k^{(i)} = [\mathbf{x}_{k,1}\ \mathbf{x}_{k,3}]$ where $\mathbf{x}_{k,\ell} = [x_{k,\ell}\ \dot{x}_{k,\ell}\ y_{k,\ell}\ \dot{y}_{k,\ell}\ I_{k,\ell}]$ is the state vector of the ℓth target, $(x_{k,\ell}, y_{k,\ell})$ and $(\dot{x}_{k,\ell}, \dot{y}_{k,\ell})$ are the two-dimensional (2-D) target position and velocity Cartesian coordinates, respectively, and $I_{k,\ell}$ depends on the RCS of the ℓth target at time step k. All targets assume the same state space representation, which, for the ℓth target, is given as $\mathbf{x}_{k,\ell} = \mathbf{f}(\mathbf{x}_{k-1,\ell}) + \mathbf{v}_{k-1,\ell}$, where $\mathbf{f}(\cdot)$ is the state transition function and $\mathbf{v}_{k-1,\ell}$ is the modeling error random process with covariance matrix $\mathbf{Q}$.

The measurements include the pre-processed radar cross section (RCS) return for different range $r_{k,\ell}$, range-rate $\dot{r}_{k,\ell}$ and azimuth angle $\theta_{k,\ell}$ bins. The measurements model is $r_{k,\ell} = ((x_{k,\ell} - x_s)^2 + (y_{k,\ell} - y_s)^2)^{0.5}$, $\dot{r}_{k,\ell} = [\dot{x}_{k,\ell}(x_{k,\ell} - x_s) + \dot{y}_{k,\ell}(y_{k,\ell} - y_s)]/r_{k,\ell}$, and $\theta_{k,\ell} = \arctan((y_{k,\ell} - y_s)/(x_{k,\ell} - x_s))$, where (x_s, y_s) is the 2-D sensor location. Each measurement frame consists of $N_r \times N_{\dot{r}} \times N_\theta$ bins. The range, range-rate and azimuth angle bin resolutions are denoted by Δ_r, $\Delta_{\dot{r}}$, Δ_θ, respectively. The ηth bin, $\eta = (a, b, c)$, is then centered around $a\,\Delta_r \times b\,\Delta_{\dot{r}} \times c\,\Delta_\theta$. The measurements in all the bins consist of only noise if no targets are present. If a target is present, the measurements in the bins that are in the vicinity of this target's current position consist of both signal and noise. We consider a point target and a sensor point spread function that can be approximated by a 3-D Gaussian measurement function that depends on the state of mode m_k at time step k. We also consider a target indicator function, $C_\ell^i = q$, $i = 0, 1, \ldots M-1$, where q is 1 (or 0) if the ℓth target is present (not present) in mode i. Based on this, the measurement equation is given by

$$z_k^{(\eta)} = \begin{cases} \displaystyle\sum_{\ell=1}^{\mathtt{L}} C_\ell^i\, h_k^{(\eta)}(\mathbf{x}_{k,\ell}) + v_k^{(\eta)}, & i \neq 0 \\ v_k^{(\eta)}, & i = 0 \end{cases} \tag{1}$$

with Gaussian $h_k^{(\eta)}(\mathbf{x}_{k,\ell}) = A_k \exp\big(\big(\frac{a\Delta_r - r_{k,\ell}}{2\sigma_r}\big)^2 - \big(\frac{b\,\Delta_{\dot{r}} - \dot{r}_{k,\ell}}{2\sigma_{\dot{r}}}\big)^2 - \big(\frac{c\,\Delta_\theta - \theta_{k,\ell}}{2\sigma_\theta}\big)^2\big)$, $A_k = (\Delta_r \Delta_{\dot{r}} \Delta_\theta I_{k,\ell})/((2\pi)^{3/2}\sigma_r\sigma_{\dot{r}}\sigma_\theta)$ is the normalized amplitude, $I_{k,\ell}$ is a function of the ℓth target amplitude, and $\sigma_r, \sigma_{\dot{r}}, \sigma_\theta$ are known spreading control parameters. The noise samples $v_k^{(\eta)}$ in (1) are assumed to be white Gaussian with zero-mean and variance ν_k. The overall measurement vector is given by $\mathbf{z}_{k,s} = [z_{k,s}^{(1,1,1)}\ \ldots\ \ldots\ z_{k,s}^{(1,N_{\dot{r}},N_\theta)}\ \ldots\ z_{k,s}^{(N_{\dot{r}},N_{\dot{r}},N_\theta)}]^{\mathtt{T}}$, $\mathbf{z}_k = \{\mathbf{z}_{k,1}, \ldots, \mathbf{z}_{k,S}\}$ is the set of measurements from S independent and homogeneous sensors, and $\mathbf{Z}_k = \{\mathbf{z}_1, \ldots, \mathbf{z}_k\}$ represents all the measurements up to time k.

III. MULTIPLE-MODE MULTIPLE-TARGET TBD

The MMMT-TBD algorithm computes the posterior PDF of the joint target state vector conditioned on a mode; for mutually exclusive modes, it can be written as

$$p(\mathbf{x}_{k,\ell}|\mathbf{Z}_k) = \sum_{i=0}^{M-1} C_\ell^i\ p(\mathbf{x}_{k,l},\, m_{k,i}|\mathbf{Z}_k).$$

where $m_{k,i}$ represents $m_k = i$ (mode m_k is i at time step k). The PDF $p(\mathbf{x}_{k,l}, m_{k,i}|\mathbf{Z}_k)$ is obtained by marginalizing the joint PDF as $p(\mathbf{x}_k^{(i)}, m_{k,i}|\mathbf{Z}_k) = p(\mathbf{x}_k^{(i)}|m_{k,i}, \mathbf{Z}_k)\,\Pr(m_{k,i})$, where $\Pr(m_{k,i}) \triangleq \Pr(m_{k,i}|\mathbf{Z}_k)$. The target state PDF conditioned on mode i is

$$p(\mathbf{x}_k^{(i)}|m_{k,i}, \mathbf{Z}_k) = \sum_{j=0}^{M-1} p_{j,i}(\mathbf{x}_k^{(i)}|\mathbf{Z}_k)\ \Pr(m_{k,i|j})\,. \tag{2}$$

where $p_{j,i}(\mathbf{x}_k^{(i)}|\mathbf{Z}_k) = p(\mathbf{x}_k^{(i)}|m_{k-1,j}, m_{k,i}, \mathbf{Z}_k)$ is the posterior PDF conditioned on the mode transitioning from j at time $k-1$ to i at time k, and $\Pr(m_{k,i|j}) = \Pr(m_{k,i}|m_{k-1,j}, \mathbf{Z}_k)$. Using TBD, $p_{j,i}(\mathbf{x}_k^{(i)}|\mathbf{Z}_k)$ can be expressed in terms of likelihood ratios as [13]

$$p_{j,i}(\mathbf{x}_k^{(i)}|\mathbf{Z}_k) = L_{j,i}(\mathbf{z}_k|\mathbf{x}_k^{(i)})\ p_{j,i}(\mathbf{x}_k^{(i)}|\mathbf{Z}_{k-1})/\Lambda_{j,i}$$

where $\Lambda_{j,i} = L_{j,i}(\mathbf{z}_k|\mathbf{Z}_{k-1})$ is a normalization factor obtained by integrating the numerator, $L_{j,i}(\mathbf{z}_k|\mathbf{x}_k^{(i)}) = 1$ if $m_k = 0$, $L_{j,i}(\mathbf{z}_k|\mathbf{x}_k^{(i)}) = \prod_\eta \lambda(z_k^{(\eta)}|\mathbf{x}_k^{(i)})$ if $m_k, m_{k-1} \neq 0$, $\lambda(z_k^{(\eta)}|\mathbf{x}_k^{(i)}) = \exp(-\Upsilon_k^{(\eta)}(\mathbf{x}_k^{(i)})(\Upsilon_k^{(\eta)}(\mathbf{x}_k^{(i)}) - 2z_k^{(\eta)}/(2\nu_k))$, and $\Upsilon_k^{(\eta)}(\mathbf{x}_k^{(i)}) = \sum_{\ell=1}^{\mathtt{L}} C_\ell^i\, h_k^{(\eta)}(\mathbf{x}_{k,\ell})$. The weights are computed using $\Pr(m_{k,i|j}) = A_{i,j}/(\sum_{j'=0}^{M-1} A_{i,j'})$, where $A_{i,j} = \Lambda_{j,i}\,\mathbf{\Phi}_{j,i}\Pr(m_{k-1,j})$. The posterior mode probability is $\Pr(m_{k,i}) = (\sum_{j=0}^{M-1} A_{i,j})/(\sum_{j=0}^{M-1}\sum_{i'=0}^{M-1} A_{i',j})$. The recursive TBD for one target ($\mathtt{L} = 1$) is a special case of MMMT-TBD [15].

IV. PF IMPLEMENTATION OF MMMT-TBD

Since the measurement model is highly nonlinear, MMMT-TBD is implemented using 3 PFs that approximate the posterior PDFs $p_{j,i}(\mathbf{x}_k^{(i)}|\mathbf{Z}_k)$, $p(\mathbf{x}_k^{(i)}|m_{k,i}, \mathbf{Z}_k)$ and $p(\mathbf{x}_{k,\ell}|\mathbf{Z}_k)$ using particles and weights $\{\mathbf{x}_k^{(j,i,n)}, \psi_k^{(j,i,n)}\}$, $n = 1, \ldots, N_{j,i}$, $\{\mathbf{x}_k^{(i,n)}, \chi_k^{(i,n)}\}$, $n = 1, \ldots, N_i$, and $\{\mathbf{x}_{k,\ell}^{(n)}, w_k^{(n)}\}$, $n = 1, \ldots, N_\ell$, respectively. The particles $\mathbf{x}_0^{(i,n)}$ and weights $\chi_0^{(i,n)}$ for the ith mode are assumed to be initialized. At time step k, $N_{j,i}$ new particles are generated to approximate the predicted posterior PDF $p_{j,i}(\mathbf{x}_k^{(i)}|\mathbf{Z}_{k-1})$ based on 3 possible target transitions: (a) if the target in mode i is absent in mode j, the particles are generated from a uniform distribution if no prior information is available; (b) if the target is present in mode j but not in mode i, the particles at time $k-1$ are ignored at time k; (c) if the target is present in modes i and j, the particles are updated using the state transition model. The particles from all targets in mode i are concatenated to approximate $p_{j,i}(\mathbf{x}_k^{(i)}|\mathbf{Z}_{k-1})$.

If the targets are moving independently, then the weights for $p_{j,i}(\mathbf{x}_k^{(i)}|\mathbf{Z}_k)$ are computed using,

$$\tilde{\psi}_k^{(j,i,n)} \propto L_{j,i}(\mathbf{z}_k|\mathbf{x}_k^{(i)}) \prod_{\ell=1}^{\mathtt{L}_\mathtt{i}} \frac{p(\mathbf{x}_{k,\ell}^{(j,i,n)}|\mathbf{x}_{k-1,\ell}^{(j,i,n)}, \mathbf{Z}_k)}{q(\mathbf{x}_{k,\ell}^{(j,i,n)}|\mathbf{x}_{k-1,\ell}^{(j,i,n)}, \mathbf{Z}_k)}$$

where $q(\cdot)$ is the proposal function used to generate the particles. The weights are normalized by $\Lambda'_{j,i} = \sum_{n=0}^{N_{j,i}} \tilde{\psi}_k^{(j,i,n)}$ to obtain $\psi_k^{(j,i,n)} = \tilde{\psi}_k^{(j,i,n)}/\Lambda'_{j,i}$, where $\Lambda'_{j,i}$ is the particle approximation of $\Lambda_{j,i}$. Given the initial mode probability $\Pr(m_{0,i})$, the mixing probabilities $\Pr(m_{k,i|j})$ are calculated given the initial mode probability $\Pr(m_{0,i})$. The posterior PDF $p(\mathbf{x}_k^{(i)}|m_{k,i}, \mathbf{Z}_k)$ in Equation (2) is then approximated as

$$p(\mathbf{x}_k^{(i)}|m_{k,i}, \mathbf{Z}_k) \approx \sum_{j=0}^{M-1}\sum_{n=1}^{N_{j,i}} \tilde{\chi}_k^{(j,i,n)}\ \delta(\mathbf{x}_k^{(i)} - \mathbf{x}_k^{(j,i,n)})\,,$$

where $\tilde{\chi}_k^{(j,i,n)} = \Pr(m_{k,i|j})\psi_k^{(j,i,n)}$. The number of particles representing $p(\mathbf{x}_k^{(i)}|m_{k,i}, \mathbf{Z}_k)$ is the sum of particles from all modes that transition to mode i. To avoid an exponential increase in particles, the weights are sorted and the N_i highest weights and corresponding particles are selected. The sorted weights are then normalized and resampled to obtain $\chi_k^{(i,n)}$. The mode probabilities are computed by substituting $\Lambda'_{j,i}$ for $\Lambda_{j,i}$. The mode probability when no targets are present is obtained using $\Pr(m_{k,0})=1-\sum_{i=1}^{M-1}\Pr(m_{k,i})$. The particles from all the modes that include the ℓth target are combined and weighted according to the mode probability. The marginal PDF of the ℓth targets is obtained by selecting particles corresponding to the ℓth target from all modes

$$p(\mathbf{x}_{k,\ell}|\mathbf{Z}_k) \approx \sum_{i=1}^{M-1}\sum_{n=1}^{N_i} C_\ell^i \Pr(m_{k,i})\ \chi_k^{(i,n)}\ \delta(\mathbf{x}_{k,\ell}^{(i)} - \mathbf{x}_{k,\ell}^{(i,n)})\,. \quad (3)$$

The number of particles used in (3) is the sum of all particles from modes that contains the ℓth target. The weights are then sorted, and the N_ℓ largest weights with corresponding particles are selected. The sorted weights are then normalized and resampled to obtain $w_{k,\ell}^{(n)}$. Finally, the target existence probability of the ℓth target is obtained by summing up the relevant mode probabilities as $\sum_{i=1}^{M-1} C_\ell^i \Pr(m_{k,i})$.

V. PROPOSAL USING PARTITIONED SAMPLING

One of the MMMT-TBD drawbacks is the large number of necessary PF computations, that increases with the number of targets. In [16], a method was used to estimate the joint multi-target PDF for tracking an unknown number of targets. Different proposal methods were considered by partitioning the single target state space; this resulted in reducing the number of particles using measurements to generate proposal particles. We propose an approach using the measurements during particle generation for the posterior PDF $p_{j,i}(\mathbf{x}_k^{(i)}|\mathbf{Z}_k)$ and the sequential independent partitioning (IP) algorithm to exploit the fact that the number of targets in a mode is known. Under this assumption, the number of partitions in a mode is the same as the number of targets.

There are five main steps in the sequential independent partition (IP) algorithm [16], [17]: partition sampling, partition weight computation, resampling of partition weights, particle weights computation, and particle resampling. In the previous section, we approximated the predicted posterior PDF $p_{j,i}(\mathbf{x}_k^{(i)}|\mathbf{Z}_{k-1})$ using new and surviving particles. Using partitions, the likelihood function corresponding to the predicted particles for each target in a mode is computed first, this function corresponds to the partition weights $\alpha_{k,\ell}^{(j,i,n)}$, which are normalized and resampled to generate a new set of predicted particles. Assuming that the targets are moving independently, the joint proposal can be written as

$$q(\mathbf{x}_k^{(j,i,n)}|\mathbf{x}_{k-1}^{(j,i,n)},\mathbf{Z}_k) = \prod_{l=1}^{\mathtt{L_i}} q(\mathbf{x}_{k,\ell}^{(j,i,n)}|\mathbf{x}_{k-1,\ell}^{(j,i,n)},\mathbf{Z}_k)\,, \quad (4)$$

where $\mathtt{L_i}$ is the number of targets in mode i. Since the proposal function now depends also on the measurement likelihood, the proposal functions for a target entering the FOV and surviving are given, respectively, by [17]

$$q_{\text{ent}}(\mathbf{x}_{k,\ell}^{(j,i,n)}|\mathbf{x}_{k-1,\ell}^{(j,i,n)},\mathbf{Z}_k) = \alpha_{k,\ell}^{(j,i,n)}\ q(\tilde{\mathbf{x}}_{k,\ell}^{(j,i,n)})$$

$$q_{\text{sur}}(\mathbf{x}_{k,\ell}^{(j,i,n)}|\mathbf{x}_{k-1,\ell}^{(j,i,n)},\mathbf{Z}_k) = \alpha_{k,\ell}^{(j,i,n)}\ p(\tilde{\mathbf{x}}_{k,\ell}^{(j,i,n)}|\mathbf{x}_{k-1,\ell}^{(j,i,n)})\,.$$

Algorithm 1 Partition-based Proposal Sampling Algorithm

Step 1: Predict the particle distribution for $p_{j,i}(\mathbf{x}_k^{(i)}|\mathbf{Z}_{k-1})$
- New entering target for lth partition $\mathbf{x}_{k,\ell}^{(j,i,n)} \sim q(\tilde{\mathbf{x}}_{k,\ell}^{(j,i,n)})$
- Surviving target: $\tilde{\mathbf{x}}_{k,\ell}^{(j,i,n)} \sim p(\tilde{\mathbf{x}}_{k,\ell}^{(j,i,n)}|\mathbf{x}_{k-1,\ell}^{(j,i,n)})$
- Partition weights: $\alpha_{k,\ell}^{(j,i,n)} \propto p(\mathbf{Z}_k|\tilde{\mathbf{x}}_{k,\ell}^{(j,i,n)})$
- Normalize weigths: $\alpha_{k,\ell}^{(j,i,n)} = \alpha_{k,\ell}^{(j,i,n)}/\sum_{n=1}^{N_{j,i}}\alpha_{k,\ell}^{(j,i,n)}$
- Resample normalized particles: $\{\mathbf{x}_{k,\ell}^{(j,i,n)},\alpha_{k,\ell}^{(j,i,n)}\}$
- Concatenate new particles from all partitions: $\mathbf{x}_k^{(j,i,n)}$

Step 2: Compute weights using the proposal function in (4)
$\tilde{\psi}_k^{(j,i,n)} = L(\mathbf{z}_k|\mathbf{x}_k^{(j,i,n)}, m_{k-1,j}, m_{k,i})/(N_{j,i}\prod_{\ell=1}^{\mathtt{L_i}}\alpha_{k,\ell}^{(j,i,n)})$

The steps of the resulting MMMT-TBD-IP algorithm are summarized in Algorithm 1. In order to reduce the PF sample impoverishment, we employ a Metropolis-Hastings (MH) Markov chain Monte Carlo step (MMMT-TBD-MH) after the proposal particle generation, as described in [3].

VI. SIMULATIONS

For our simulations, we assume constant velocity target motion and additive Gaussian process error and noise models. We consider a (5×5) state model matrix $\mathbf{f}$ in Section II defined to be 0 everywhere except the diagonal values $\mathbf{f}_{ii}=1$, $i=1,\ldots 5$, and $\mathbf{f}_{34}=\mathbf{f}_{12}=\delta t$, where δt is the duration between time steps. The (5×5) modeling error covariance matrix $\mathbf{Q}$ has entries $\mathbf{Q}_{11}=\mathbf{Q}_{33}=q_1\,\delta t^4/4$, $\mathbf{Q}_{12}=\mathbf{Q}_{21}=q_1\,\delta t^3/2$, $\mathbf{Q}_{43}=\mathbf{Q}_{34}=q_1\,\delta t^3/2$, $\mathbf{Q}_{22}=\mathbf{Q}_{44}=q_1\,\delta t^2$, $\mathbf{Q}_{55}=q_2\,\delta t$, where q_1 and q_2 are modeling error parameters for motion and intensity, respectively; all other $\mathbf{Q}$ entries are 0. For the simulations, we set $q_1=0.01$ and $q_2=0.001$. The FOV is set to 0 m and 16.97 m in the x and y directions, respectively. The measurements are obtained from two sensors located at (0, 0) and (0, 16.97) m. A single measurement frame consists of $48\times48\times48$ bins, resulting in bin resolutions of $\Delta_r=0.509$ m, $\Delta_{\dot r}=0.0766$ m/s, and $\Delta_\theta=0.0334$ radians. The measurements range in value between [0 24) m for range, [-1.8 1.8) m/s for range-rate, and $[0\ \pi/2)$ radians for azimuthal angles for Sensor 1 and $(-\pi/2\ 0]$ radians for Sensor 2. The transmission matrix is selected as $\Pr_{\mathrm{B},1}=\Pr_{\mathrm{D},1}=0.02$. The spread factors are set to $\sigma_r=1.1$ m , $\sigma_{\dot r}=0.35$ m/s, and $\sigma_\theta=0.06$ radians. The measurement noise variance ν_k is set to 1. The peak SNR at time step k corresponding to the ℓth target is calculated as $(\Delta_r\Delta_{\dot r}\Delta_\theta I_{k,\ell})^2/((2\pi)^{3/2}\sigma_r\sigma_{\dot r}\sigma_\theta)^2\,\nu_k)$. Figure 1(a) demonstrates the instantaneous peak SNRs for 3 targets that enter and leave the FOV at different times; this value is sometimes lower than the predetermined peak SNR due to the discretization needed to obtain the measurement bins. In the first simulation, the measurements were generated at 3 dB peak SNR for 3 targets that enter the FOV at frames 5, 13, 21 and leave at frames 25, 33, 41, respectively. The initial positions and velocities for each of the 3 targets are (4.2, 1.2) m and (0.35, 0.70) m/s, (16.2, 2.2) m and (-0.70, 0.15) m/s, and (1.2, 16.2) m and (0.65, -0.45) m/s, respectively.

In the simulations, after the state and measurement model attributes are selected, the following parameters are chosen. The mutitarget tracking performance is evaluated using the cardinality and

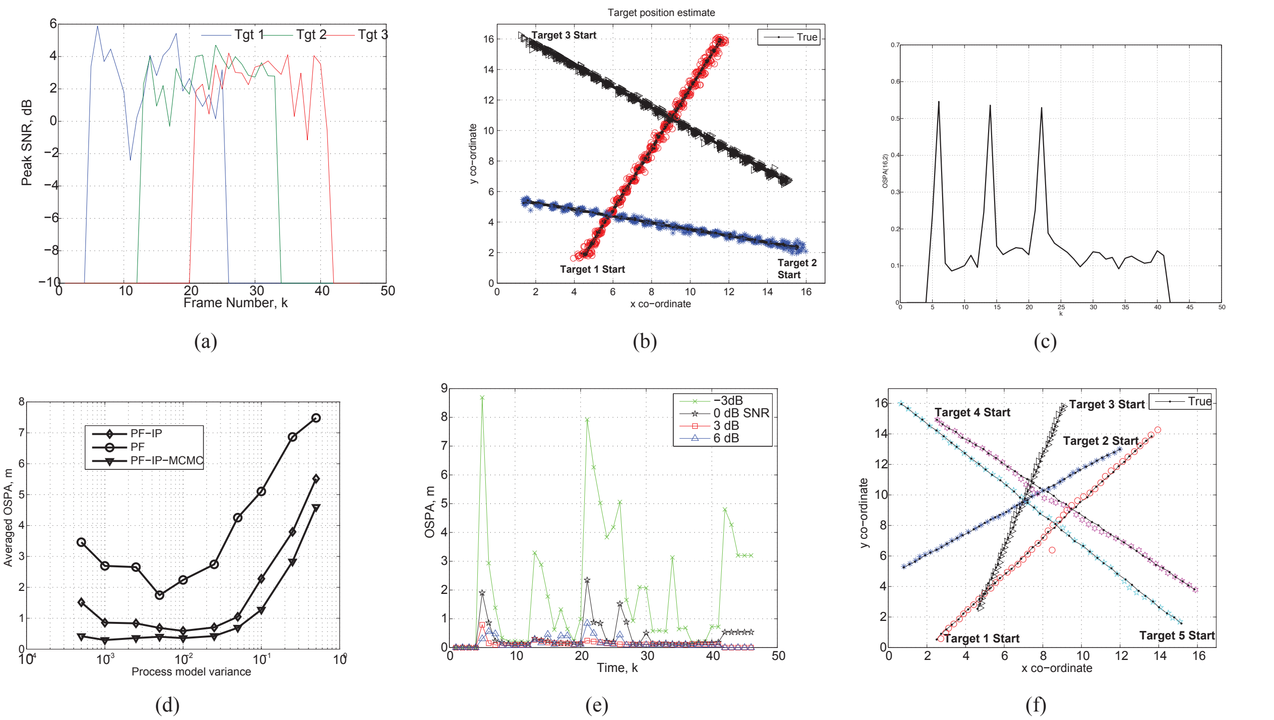

Fig. 1. Three targets: (a) instantaneous peak SNR; (b) true and estimated trajectories at 3 dB peak SNR; (c) OSPA(16, 2) at 3 dB peak SNR; OSPA versus (d) process model variance and (e) peak SNR; (f) true and estimated trajectories of 5 targets at 3 dB peak SNR.

localization error obtained from the optimal sub-pattern assignment (OSPA) metric [18]. The OSPA cut-off parameter value c is set to $c = 16$, chosen to be in the same order as the FOV; the OSPA parameter $p = 2$. The numbers of particles ($N_{j,i}$, N_i and N_ℓ) are set to 500 for all PFs. The number of Monte-Carlo (MC) simulations run is 30.

Figure 1(b) shows the estimated and true target trajectories (plotted using solid lines). Note that the estimated target location deviates initially from the true location; however, the estimate converges to the true location as more measurements are received. Figure 1(b) shows the OSPA metric averaged over 30 MC simulations. The cardinality error dominates the OSPA during the onset of target appearance; thus, there is one frame latency in detecting a target entering the FOV. On the other hand, targets exiting the FOV are detected correctly. The localization error is only around 0.1 m.

Using a similar set for the second set of simulations, we compared the performances of the three multi-target tracking algorithms discussed in the paper, MMMT-TBD, MMMT-TBD-IP and MMMT-TBD-MH, for various process model noise variance values q_1. The averaged OSPA over all MC simulations is again averaged across time to obtain a single OSPA value. Figure 1(d) compares the averaged OSPA for different values of q_1. As expected, for the same number of particles, the averaged OSPA with the IP method is higher for smaller process model variance values. The error introduced by the sample impoverishment is improved using the MCMC steps; the OSPA from the MMMT-TBD-MH algorithm has the smallest value when compared to that of the other two methods for all q_1. Figure 1(e) shows the OSPA at different peak SNR conditions. The proposed MMMT-TBD-MH algorithm tends to fall apart at -3 dB peak SNR as the cardinality error at every mode transition is very high, in addition to the large localization errors present.

The third simulation shows tracking results for five targets. The initial positions and velocities for each of the targets were (2.2, 0.2) m and (0.28, 0.33) m/s, (12.2, 13.2) m and (-0.38,-0.19) m/s, and (9.2, 16.2) m and (-0.11, -0.33) m/s, and (2.2, 15.2) m and (0.33, -0.28) m/s, and (15.5, 1.2) m and (-0.36, 0.36) m/s, respectively. The entering and leaving frames for each target are 5 & 45 for Target 1, 11 & 51 for Target 2, 17 & 57 for Target 3, 23 & 63 for Target 4, and 29 & 69 for Target 5. Figure 1(f) shows the true and estimated trajectories for the five closely-spaced targets at 3 dB peak SNR. The trajectory of Target 5 deviates somewhat at around (7.8,10) m due to the presence of the other targets, but it re-converges to the true path after some delay.

VII. CONCLUSION

We derived a partition-based multiple transition mode algorithm using track-before-detect for tracking multiple targets under low SNR conditions, and we implemented it using sequential Monte Carlo techniques. The different transition modes keep track of targets entering or leaving the FOV, and only the maximum number of targets needs to be assumed known; this number can be assumed large, based on the application. The algorithm performs well for a larger number of targets than was demonstrated in previous works.

VIII. REFERENCES

[1] Y. Bar-Shalom and X.-R. Li, *Multisensor Tracking: Principles and Techniques*. New York: YBS Publishing, 1995.

[2] R. P. S. Mahler, "Multitarget Bayes filtering via first-order multitarget moments," *IEEE Transactions on Aerospace and Electronic Systems*, vol. 39, no. 2, pp. 1152–1178, 2003.

[3] B. Ristic, S. Arulampalam, and N. Gordon, *Beyond the Kalman Filter: Particle Filters for Tracking Applications*. Artech House, 2004.

[4] M. G. Rutten, N. J. Gordon, and S. Maskell, "Efficient particle-based track-before-detect in Rayleigh noise," in *International Conference on Information Fusion*, June 2004.

[5] H. Driessen and Y. Boers, "An efficient particle filter for nonlinear jump Markov systems," in *IEE Seminar on Target Tracking: Algorithms and Applications*, March 2004.

[6] M. Taj and A. Cavallaro, "Multi-camera track-before-detect," in *IEEE Int. Conf. Distr. Smart Cameras*, Sept. 2009, pp. 1–6.

[7] P. Pertilä and M. S. Hämäläinen, "A track before detect approach for sequential Bayesian tracking of multiple speech sources," in *IEEE Int. Conf. Acoustics, Speech, Signal Processing*, 2010, pp. 4974–4977.

[8] K. Punithakumar, T. Kirubarajan, and A. Sinha, "A sequential Monte Carlo probability hypothesis density algorithm for multitarget track-before-detect," *Proc. SPIE*, vol. 5913, 2005.

[9] B. K. Habtemariam, R. Tharmarasa, and T. Kirubarajan, "PHD filter based track-before-detect for MIMO radars," *Signal Processing*, vol. 92, no. 3, pp. 667–678, March 2012.

[10] H. Tong, H. Zhang, H. Meng, and X. Wang, "Multitarget tracking before detection via probability hypothesis density filter," in *Electr. Control Eng.*, 2010, pp. 1332–1335.

[11] R. Zhan and J. Zhang, "Improved multitarget track-before-detect for image measurements," in *Int. Conf. Signal Processing*, vol. 3, 2012, pp. 2183–2187.

[12] B.-N. Vo, S. Singh, and A. Doucet, "Sequential Monte Carlo methods for multitarget filtering with random finite sets," *Aerospace and Electronic Systems, IEEE Transactions on*, vol. 41, no. 4, pp. 1224–1245, 2005.

[13] S. P. Ebenezer and A. Papandreou-Suppappola, "Multiple mode track-before-detect for multiple targets," in *Int. Waveform Design and Diversity Conference*, January 2012.

[14] Y. Boers and H. Driessen, "Multitarget particle filter track before detect application," *IEE Proceedings of Radar, Sonar and Navigation*, vol. 151, pp. 351–357, December 2004.

[15] M. G. Rutten, N. J. Gordon, and S. Maskell, "Recursive track-before-detect with target amplitude fluctuations," in *IEE Proceedings of Radar, Sonar and Navigation*, vol. 52, October 2005, pp. 345–352.

[16] C. Kreucher, K. Kastella, and A. Hero, "Multitarget tracking using the joint multitarget probability density," *IEEE Trans. Aerospace Elect. Syst.*, vol. 41, pp. 1396–1414, 2005.

[17] I. Kyriakides, D. Morrell, and A. Papandreou-Suppappola, "Sequential Monte Carlo methods for tracking multiple targets with deterministic and stochastic constraints," *IEEE Transactions on Signal Processing*, vol. 56, pp. 937–948, March 2008.

[18] D. Schuhmacher, B.-T. Vo, and B.-N. Vo, "A consistent metric for performance evaluation of multi-object filters," *IEEE Trans. Signal Processing*, vol. 56, pp. 3447–3457, 2008.